Acta Crystallographica Section D
Biological Crystallography
ISSN 0907-4449

Purification, crystallization and preliminary X-ray analysis of *Escherichia coli* UDP-*N*-acetylmuramoyl:L-alanine ligase (MurC)

Taru Deva,[a] KellyAnn D. Pryor,[b] Barbara Leiting,[b] Edward N. Baker[a] and Clyde A. Smith[a]*

[a]Laboratory of Structural Biology, School of Biological Sciences, University Of Auckland, Auckland, New Zealand, and [b]Department of Endocrinology and Chemical Biology, Merck Research Laboratories, Rahway, NJ 07065, USA

Correspondence e-mail: ca.smith@auckland.ac.nz

Received 22 March 2003
Accepted 10 June 2003

UDP-*N*-acetylmuramoyl:L-alanine ligase (MurC) is involved in the pathway leading from UDP-*N*-glucosamine to the UDP-*N*-acetylmuramoyl:pentapeptide unit, which is the building block for the peptidoglycan layer found in all bacterial cell walls. The pathways leading to the biosynthesis of the peptidoglycan layer are important targets for the development of novel antibiotics, since animal cells do not contain these pathways. MurC is the first of four similar ATP-dependent amide-bond ligases which share primary and tertiary structural similarities. The crystal structures of three of these have been determined by X-ray crystallography, giving insights into the binding of the carbohydrate substrate and the ATP. Diffraction-quality crystals of the enzyme MurC have been obtained in both native and selenomethionine forms and X-ray diffraction data have been collected at the Se edge at a synchrotron source. The crystals are orthorhombic, with unit-cell parameters $a = 73.9$, $b = 93.6$, $c = 176.8$ Å, and diffraction has been observed to 2.6 Å resolution.

1. Introduction

The strength and rigidity of the cell wall of both Gram-positive and Gram-negative bacteria primarily arises from the presence of a layer of peptidoglycan. The basic structure of this molecule is a thin sheet of glycan chains connected by short cross-linking polypeptides. In Gram-positive bacteria up to 90% of the cell wall can consist of peptidoglycan, in contrast to Gram-negative bacteria where it contributes only about 10% of the wall, sandwiched between the cytoplasmic and periplasmic membranes (Madigan *et al.*, 1997). Biosynthesis of peptidoglycan is a multi-step process comprising three main stages: (i) biosynthesis of UDP-*N*-acetylmuramic acid (UDP-MurNAc), (ii) addition of a pentapeptide chain to the UDP-MurNAc and (iii) transport of this unit through the cytoplasmic membrane and incorporation into the growing peptidoglycan layer (van Heijenoort, 1994, 2001). UDP-MurNAc is formed from UDP-*N*-acetylglucosamine in two steps: addition of phosphoenolpyruvate catalysed by the enzyme UDP-*N*-acetylglucosamine enolpyruvyl transferase (MurA) and subsequent reduction of the enolpyruvyl group to lactate by UDP-*N*-acetylpyruvyl-glucosamine reductase (MurB). The pentapeptide chain is then added sequentially by four enzymes: UDP-*N*-acetylmuramoyl:L-alanine ligase (MurC), UDP-*N*-acetylmuramoyl-L-alanine:D-glutamate ligase (MurD), UDP-*N*-acetylmuramoyl-L-alanine-D-glutamate:*meso*-diaminopimelate ligase (MurE) and UDP-*N*-acetylmuramoyl-L-alanine-D-glutamate-*meso*-diaminopimelate:D-alanyl-D-alanine ligase (MurF). These four enzymes have a similar enzymatic mechanism involving the activation of the free caroxylate by phosphoryl transfer from ATP, forming an acyl phosphate intermediate (Anderson *et al.*, 1996), followed by formation of a new amide bond with the incoming amino acid. These enzymes show a limited sequence identity of between 15 and 22%, although several regions of high sequence identity have been observed in the four cell-wall ligases (Bouhss *et al.*, 1997; Eveland *et al.*, 1997) and in other members of the ATP-dependent amide-bond ligase superfamily, including folylpolyglutamate synthetase (FPGS; Sheng *et al.*, 2000) and cyanophycin synthetase (Bertrand *et al.*, 2000).

The crystal structures of a number of these enzymes are known, including MurA from *Enterobacter cloacae* (Schonbrunn *et al.*, 1996) and *Escherichia coli* (Skarzynski *et al.*, 1996), MurB from *E. coli* (Benson *et al.*, 1995) and *Staphylococcus aureus* (Benson *et al.*, 2001) and the *E. coli* ligases MurD (Bertrand *et al.*, 1997, 1999, 2000), MurE (Gordon *et al.*, 2001), and MurF (Yan *et al.*, 2000). A model for MurC from *Thermatoga maritima* has been deposited in the Protein Data Bank (PDB code 1j6u), but is yet to be published. The three published ligases all share a common architecture. They are composed of three structural domains: an N-terminal domain primarily responsible for binding the MurNAc substrate, a central ATPase domain bearing a resemblance to the ATP-binding domains of a number of ATPases and GTPases, including myosin and ras-P21,

and a C-terminal domain possibly associated with binding the incoming amino acid (Bertrand *et al.*, 1997; Gordon *et al.*, 2001). The N-terminal domains tend to vary somewhat in structure, presumably owing to the variation in the length of the polypeptide chain that they must accommodate. The only other structure of an enzyme from this amide-bond ligase superfamily is FPGS from *Lactobacillus casei* (Sun *et al.*, 1998); this shows a similar overall structure to the cell-wall ligases (Sheng *et al.*, 2000).

The pathways involved in the biosynthesis of the bacterial cell wall are important targets for antibiotics, since animal cells do not contain peptidoglycan and hence do not possess these enzymes. Several steps in the biosynthesis of peptidoglycan have already been targeted by antibiotics, including MurA, which is inhibited by fosfomycin, a phosphoenolpyruvate analog (Skarzynski *et al.*, 1996), and more importantly the steps involved in cross-linking the polypeptide chains, which are inhibited by the β-lactam antibiotics. We have undertaken the structural analysis of MurC in order to fully understand the structural determinants which give rise to substrate specificity in the four cell-wall ligases. Although the crystallization of this enzyme from *E. coli* has been reported (Emanuele *et al.*, 1996), the structure of the enzyme has not been determined. In this paper, we report the crystallization of both the native and selenomethionine forms of *E. coli* MurC. The MurC obtained after purification had a marked tendency to aggregate and this caused problems during crystallization trials. We used dynamic light scattering (DLS) as a tool to improve the quality of the protein and obtain a fraction which could be crystallized readily and reproducibly; these data are also described here.

2. Materials and methods

2.1. Expression and purification

The *MurC* gene was amplified from K12 *Escherichia coli* DNA using the following oligonucleotides: 5′-GACATATGAATAC-ACAACAATTGGCA-3′ and 5′-GAGTC-GACTCAGTCATGTTGTTCTTCCTCC-3′. The PCR product was digested with restriction enzymes *Nde*I and *Sal*I and cloned into the pET30a(+) vector (Novagen). The final construct was verified by DNA sequencing and expressed as native MurC as given by Genbank accession code X55034.

MurC was expressed from a pET30a(+) plasmid construct. *E. coli* BL21 (DE3) cells were transformed with the construct. 200 ml of LB medium containing 25 µg ml^{-1} kanamycin was inoculated with a 2 ml starter culture and incubated at 310 K on a shaker for 3 h. The culture was induced with 0.1 m*M* IPTG and grown for another 2.5–3 h. The cells were harvested by centrifugation (7000 rev min^{-1}, 293 K, 10 min). The cell pellet was resuspended in 20 ml buffer *A* (10 m*M* bis-tris propane pH 6.7, 300 m*M* NaCl, 1.5 m*M* β-mercaptoethanol), lysed by sonication and centrifuged at 13 000 rev min^{-1} at 277 K for 10 min.

Although the use of the *Nde*I and *Sal*I restriction enzymes removes any potential His tag from the plasmid, the supernatant was loaded onto an Ni^{2+}-affinity column (Hitrap chelating column, Pharmacia) equilibrated with buffer *A* for initial purification. The column was washed with four column volumes of buffer *A* and the protein was eluted with buffer *A* containing between 5 and 500 m*M* imidazole. The fractions were analyzed by SDS–PAGE. It was found that MurC eluted at very low imidazole concentrations (10 and 20 m*M*) as expected, but this step did serve to remove a large amount of the other *E. coli* proteins prior to further purification steps. The protein was further purified using a Superdex-200 16/60 preparative column (Pharmacia) which had been equilibrated with buffer *B* (10 m*M* bis-tris propane pH 6.7, 150 m*M* NaCl, 1.5 m*M* β-mercaptoethanol). The column was eluted with buffer *B* and the fractions were once again analyzed by SDS–PAGE.

Selenomethionine-substituted MurC was produced using the methionine-biosynthesis pathway inhibition method. Cells were grown in M9 medium and the methionine pathway was inhibited by addition of Lys, Phe and Thr at 100 mg l^{-1}, and Ile, Val and Leu at 50 mg l^{-1}. L-Selenomethionine (60 mg l^{-1}) was added to compensate for the lack of methionine. The culture was induced with 0.1 m*M* IPTG after lowering the temperature to 293 K. Both native and selenomethionine-substituted MurC were concentrated using Vivaspin (polyethersulfone membrane) to a final concentration of about 10 mg ml^{-1} as measured using the Bradford protein assay (BioRAD) with BSA as the standard.

2.2. Dynamic light-scattering analysis

Dynamic light scattering (DLS) was carried out using a DynaPro (model MS) molecular-sizing instrument. Protein samples (25 µl) were centrifuged for 10 min at 13 000 rev min^{-1}, then transferred to a 12 µl quartz cuvette to measure their polydispersity. The data were analysed using the *Dynamics* software (v. 4; Moradian-Oldak *et al.*, 1988).

2.3. Crystallization

Initial crystallization trials were performed at 291 K using 96-well Crystal Clear plates (Hampton Research) and the following screens: Crystal Screen I and II, the PEG/Ion Screen (Hampton Research), an in-house PEG screen (Kingston *et al.*, 1994) and the Flexible Sparse-Matrix Screen (Zeelan, 1999). Equal volumes of protein (1 µl) and reservoir solution were mixed and placed on the platform over 50 µl of reservoir solution. Spherulites were obtained from condition 54 of the in-house PEG screen (14% mPEG 5000, 0.2 *M* bis-tris propane pH 8.5). These spherulites were used for streak-seeding into a finer screen around these conditions. Thin needles were obtained in 12–13% mPEG 5000, 0.2 *M* bis-tris propane pH 8.5. These needles were used to streak-seed again and better crystals were obtained in 2–3 d. The crystals were extremely unstable and dissolved quickly upon standing. Several different concentrations of β-mercaptoethanol and $MgCl_2$ in the reservoir were tested in order to try and stabilize the crystals. 10 m*M* β-mercaptoethanol and $MgCl_2$ were found to stabilize the native MurC crystals and larger crystals could then be obtained by serial dilution of the seeds using the hanging-drop method (Fig. 1). Crystals of selenomethionine MurC were obtained under crystallization conditions similar to those for the native crystals (12–16% mPEG 5000, 0.2 *M* bis-tris propane pH 8.3, 10 m*M* $MgCl_2$ and 50 m*M* β-mercaptoethanol) using the native crystals as primary seeds. Diffraction-quality crystals were obtained in 7–10 d.

2.4. X-ray crystallography

Single selenomethionine crystals were immersed in cryoprotectant (reservoir solu-

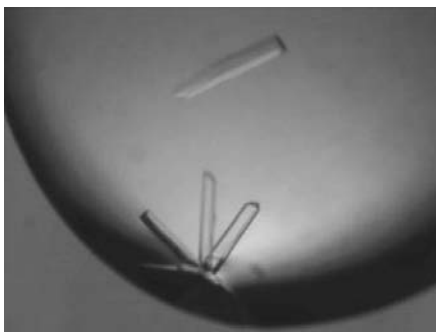

Figure 1
Single crystals of the SeMet derivative of MurC, with dimensions of approximately 0.4 × 0.1 × 0.1 mm.

Table 1
Statistics of MAD data collection.

Values in parentheses refer to the data in the highest resolution shell (2.69–2.60 Å).

	Energy (eV)	Observed reflections	Unique reflections	R_{merge}† (%)	$\langle I/\sigma(I)\rangle$	Completeness (%)
Peak	12663.6	780423	38261 (3728)	0.132 (0.667)	25.3 (3.97)	98.9 (99.8)
Inflection	12661.1	780563	38269 (3728)	0.136 (0.701)	24.9 (3.80)	99.1 (99.8)
Remote	14800.0	749744	38184 (3733)	0.133 (0.698)	23.6 (3.95)	99.3 (99.8)

† $R_{merge} = \sum |I_i - \langle I\rangle| / \sum I_i$.

tion supplemented with 20% mPEG 5000 and 20% ethylene glycol), mounted in a cryoloop and frozen immediately in liquid nitrogen. Highly redundant X-ray diffraction data were collected at the Stanford Synchrotron Radiation Laboratory (SSRL) on beamline BL9-2 using an ADSC Quantum 315 CCD detector. Three data sets were collected at the peak, inflection point and at a remote wavelength above the Se absorption edge. For all three wavelengths, 360° of data were collected using 1° oscillations and an exposure time of 25 s per image. Diffraction was typically observed to 2.6 Å resolution. Images were integrated and scaled using the *HKL* software package (Otwinowski & Minor, 1997). Some data-collection statistics are given in Table 1. The relatively high R_{merge} values obtained for the three data sets is primarily a consequence of the high redundancy (close to 20 on average for the three data sets), although some diffuse scattering is also observed at low resolution (Diederichs & Karplus, 1997). The $\langle I/\sigma(I)\rangle$ values in the highest resolution shells are close to 4, which implies that the data in this shell are still valid.

3. Results and discussion

3.1. Protein purification

E. coli MurC was expressed at a very high level and up to 100 mg of purified protein per litre of culture was obtained. DLS was used to examine all the preparations for their monodispersity. The two fractions eluted at 10 and 20 m*M* imidazole showed differing levels of polydispersity. It was found that adding β-mercaptoethanol to the fraction eluted at 10 m*M* imidazole produced protein which was monomodal and monodisperse (C_p/R_H = 7–9). These samples produced diffraction-quality crystals.

The sequence of MurC has two cysteine residues. It was found by chemical modification studies (Nosal *et al.*, 1998) that modification of one of the cysteine residues resulted in loss of activity. It has also been noted that the stability of the enzymatic activity is strictly dependent on the presence of β-mercaptoethanol (Liger *et al.*, 1996). This suggests that there is a need for the protein to be in a reducing environment at all times and that a lack of this could lead to non-native intermolecular disulfide formation and thus aggregation. Increasing the amount of β-mercaptoethanol from the beginning of the purification gave an increase in the amount of protein eluted at 10 m*M* imidazole and a decrease in the amount of protein eluting at 20 m*M* imidazole from the Ni^{2+}-affinity column. This suggests that the two bands observed at the same position on the SDS–PAGE could be MurC in different states of association or aggregation.

Stable crystallization of MurC also seems to be dependent on the presence of a reducing environment. MurC could possibly undergo inappropriate disulfide-bond formation or rearrangement as the crystallization drop becomes oxidized over time, which may lead to loss of stability of the crystals.

3.2. Crystallographic analysis of *E. coli* MurC

X-ray diffraction data using a synchrotron source have been collected from a single selenomethionine crystal for structure determination by MAD phasing. The crystal diffracted to approximately 2.6 Å resolution, with unit-cell parameters a = 73.9, b = 93.6, c = 176.8 Å and space group $P2_12_12_1$ (based upon observed systematic absences). Calculation of the Matthews coefficient (V_M; Matthews, 1968) using a molecular weight of 54 kDa gave values of 5.66 $Å^3\,Da^{-1}$ (solvent content 78%), 2.83 $Å^3\,Da^{-1}$ (solvent content 57%) or 1.89 $Å^3\,Da^{-1}$ (solvent content 35%) assuming one, two or three molecules per asymmetric unit, respectively. To determine whether non-crystallographic symmetry was present, self-rotation functions were calculated with the locked rotation-function program *GLRF* (Tong & Rossmann, 1990). No significant peaks were observed on the κ = 120° section, but the κ = 180° section showed peaks at 3.7σ consistent with the presence of a non-crystallographic twofold rotation axis. This implies the presence of a dimer in the asymmetric unit, which is consistent with the observed molecular mass of approximately 100 kDa from DLS, indicating that the active biological oligomeric state of *E. coli* MurC is most likely to also be a dimer. Since there are 14 methionine residues in MurC, this would imply that there are 28 potential selenium positions in the asymmetric unit. Determination of the selenium positions is in progress.

This work was supported by grants from the Health Research Council of New Zealand (CAS and ENB) and the Wellcome Trust (UK). The X-ray data collection was conducted at the Stanford Synchrotron Radiation Laboratory (SSRL), which is funded by the Department of Energy (BES, BER) and the National Institutes of Health (NCRR, NIGMS). We thank the staff at the SSRL for assistance, in particular Ana Gonzalez.

References

Anderson, M. S., Eveland, S. S., Onishi, H. R. & Pompliano, D. L. (1996). *Biochemistry*, **35**, 16264–16269.
Benson, T. E., Filman, D. J., Walsh, C. T. & Hogle, J. M. (1995). *Nature Struct. Biol.* **2**, 644–653.
Benson, T. E., Harris, M. S., Choi, G. H., Cialdella, J. I., Herberg, J. T., Martin, J. P. & Baldwin, E. T. (2001). *Biochemistry*, **40**, 2340–2350.
Bertrand, J. A., Auger, G., Fanchon, E., Martin, L., Blanot, D., van Heijenoort, J. & Dideberg, O. (1997). *EMBO J.* **16**, 3416–3425.
Bertrand, J. A., Auger, G., Martin, L., Fanchon, E., Blanot, D., Le Beller, D., van Heijenoort, J. & Dideberg, O. (1999). *J. Mol. Biol.* **289**, 579–590.
Bertrand, J. A., Fanchon, E., Martin, L., Chantalat, L., Auger, G., Blanot, D., van Heijenoort, J. & Dideberg, O. (2000). *J. Mol. Biol.* **301**, 1257–1266.
Bouhss, A., Mengin-Lecreulx, D., Blanot, D., van Heijenoort, J. & Parquet, C. (1997). *Biochemistry*, **36**, 11556–11563.
Diederichs, K. & Karplus, P. A. (1997). *Nature Struct. Biol.* **4**, 269–275.
Emanuele, J. J., Jin, H., Jacobson, B. L., Chang, C. Y., Einspahr, H. M. & Villafranca, J. J. (1996). *Protein Sci.* **5**, 2566–2574.
Eveland, S. S., Pompliano, D. L. & Anderson, M. S. (1997). *Biochemistry*, **36**, 6223–6229.
Gordon, E., Flouret, B., Chantalat, L., van Heijenoort, J., Mengin-Lecreulx, D. & Dideberg, O. (2001). *J. Biol. Chem.* **276**, 10999–11006.
Heijenoort, J. van (1994). *Bacterial Cell Wall*, edited by J. M. Ghuysen & R. Hakenbeck, pp. 39–54. Amsterdam: Elsevier Science.
Heijenoort, J. van (2001). *Nat. Prod. Rep.* **18**, 503–519.
Kingston, R. L., Baker, H. M. & Baker, E. N. (1994). *Acta Cryst.* D**50**, 429–440.

Liger, D., Masson, A., Blanot, D., van Heijenoort, J. & Parquet, C. (1996). *Microb. Drug Resist.* **2**, 25–27.
Madigan, M. T., Martinko, J. M. & Parker, J. (1997). *Brock Biology of Microorganisms*. Upper Saddle River, NJ, USA: Prentice Hall.
Matthews, B. W. (1968). *J. Mol. Biol.* **33**, 491–497.
Moradian-Oldak, J., Leung, W. & Fincham, A. G. (1988). *J. Struct. Biol.* **122**, 320–327.
Nosal, F., Masson, A., Legrand, R., Blanot, D., Schoot, B., van Heijenoort, J. & Parquet, C. (1998). *FEBS Lett.* **426**, 309–313.
Otwinowski, Z. & Minor, W. (1997). *Methods Enzymol.* **276**, 307–326.
Schonbrunn, E., Sack, S., Eschenburg, S., Perrakis, A., Krekel, F., Amrhein, N. & Mandelkow, E. (1996). *Structure*, **4**, 1065–1075.
Sheng, Y., Sun, X., Shen, Y., Bognar, A. L. & Smith, C. A. (2000). *J. Mol. Biol.* **302**, 427–440.
Skarzynski, T., Mistry, A., Wonacott, A., Hutchinson, S. E., Kelly, V. A. & Duncan, K. (1996). *Structure*, **4**, 1465–1474.
Sun, X., Bognar, A. L., Baker, E. N. & Smith, C. A. (1998). *Proc. Natl Acad. Sci. USA*, **95**, 6647–6652.
Tong, L. & Rossmann, M. G. (1990). *Acta Cryst.* A**46**, 783–792.
Yan, Y., Munshi, S., Leiting, B., Anderson, M. S., Chrzas, J. & Chen, Z. (2000). *J. Mol. Biol.* **304**, 435–445.
Zeelan, J. P. (1999). *Protein Crystallization: Techniques, Strategies and Tips*, edited by T. M. Bergfors, pp. 77–90. La Jolla, CA: International University Line.